Open access • Journal Article • DOI:10.1086/590133

Dating the Oldest Greenstone in India: A 3.51-Ga Precise U-Pb SHRIMP Zircon Age for Dacitic Lava of the Southern Iron Ore Group, Singhbhum Craton — Source link

Joydip Mukhopadhyay, N.J. Beukes, Richard Armstrong, Udo Zimmermann ...+2 more authors

Published on: 01 Sep 2008 - The Journal of Geology (University of Chicago Press)

Topics: Greenstone belt, Pilbara Craton, Craton, Banded iron formation and Zircon

Dating the Oldest Greenstone in India: A 3.51-Ga Precise U-Pb SHRIMP Zircon Age for Dacitic Lava of the Southern Iron Ore Group, Singhbhum Craton

Joydip Mukhopadhyay,[1] *N. J. Beukes,*[1] *R. A. Armstrong,*[2] *Udo Zimmermann,*[1,3] *Gautam Ghosh, and R. A. Medda*

Department of Geology, Presidency College, Kolkata, 86/1 College Street, Kolkata, India 700073 (e-mail: joydip17@rediffmail.com)

ABSTRACT

This article reports a precise 3506.8 ± 2.3-Ma U-Pb SHRIMP zircon age for dacitic lava in a well-preserved low-grade metamorphic and low-strained greenstone belt succession of the southern Iron Ore Group, Singhbhum craton, India. This age makes the succession the oldest-known greenstone belt succession in India and one of the oldest low-strain greenstone successions in the world after the 3.51-Ga Coonterunah Group of the Pilbara craton, Western Australia, and the moderately deformed 3.54-Ga Theespruit Formation of the Barberton Greenstone Belt, Kaapvaal craton, South Africa. The geochemical composition of the dacitic lava and related volcanic rocks suggests that they formed in a volcanic arc setting. The succession also contains a major ~120-m-thick oxide facies banded iron formation that distinguishes it from the slightly older successions of the Pilbara and Kaapvaal cratons. This banded iron formation may well be one of the oldest and most well preserved, and together with associated volcanics, it may have immediate implications for understanding >3.5-Ga surface and tectonic processes on Earth.

Introduction

Direct geochronological evidence for >3.5-Ga volcanic and sedimentary successions on Earth is scarce. These rocks occupy only a very small portion of the preserved crustal record. The best studied of the earth's oldest-known volcanosedimentary sequences are in the tectonically composite Isua Greenstone Belt, where >3800-Ma and ca. 3710-Ma sequences are juxtaposed (e.g., Compston et al. 1986; Nutman et al. 1997; see reviews in Condie 2007). Metavolcanic and sedimentary rocks of similar age but not necessarily correlated with those at Isua occur in northern Quebec (Dauphas et al. 2007), southern Greenland, and northern Labrador (see Nutman et al. 1989, 2004). The Theespruit Formation of the Onverwacht Group (Lowe 1999), Barberton Greenstone Belt, South Africa (3531 ± 10 Ma [Armstrong et al. 1990], 3511 ± 3 Ma, and 3547 ± 3 Ma [Kröner et al. 1992, 1996]), and the Coonterunah Group, Pilbara craton, Western Australia (3515.2 ± 2.7 Ma; Buick et al. 1995), are the only other volcanosedimentary successions that record the remnants of early crust >3.51 Ga. Here we report on a precise 3506.8 ± 2.3-Ma U-Pb SHRIMP zircon age from dacitic volcanic rocks from a well-preserved greenstone belt succession forming part of the Iron Ore Group (IOG) of the Singhbum craton in eastern India (fig. 1). All of the other >3.5-Ga greenstone successions, apart from the Coonterunah Group and parts of the greenstone successions in the Theespruit Formation, are generally highly strained and metamorphosed to amphibolite grade and beyond (Nutman et al. 1989, 2004; Lowe 1999; Dauphas et al. 2007), with rare and tiny low-strain enclaves still of amphibolite grade and only very locally preserved (Polat and Frei 2005). The southern IOG greenstone succession we report here is, for the most part, low

Manuscript received November 28, 2007; accepted May 16, 2008.

[1] Paleoproterozoic Mineralization Research Group, Department of Geology, University of Johannesburg, Auckland Park 2006, Johannesburg, South Africa.

[2] Research School of Earth Sciences, Australian National University, Canberra, Australian Capital Territory 0200, Australia.

[3] Department of Petroleum Engineering, University of Stavanger, 4036 Stavanger, Norway.

[The Journal of Geology, 2008, volume 116, p. 449–461] 0022-1376/2008/11605-0002$15.00 DOI: 10.1086/590133

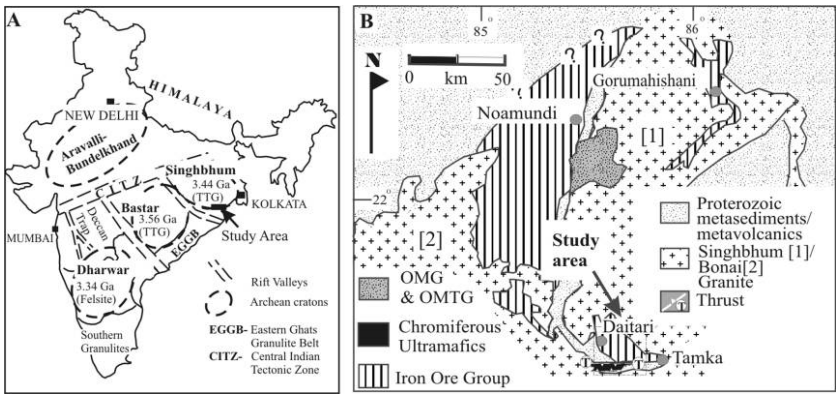

Figure 1. *A*, Three major cratonic nuclei separated by major rift valleys in the Indian subcontinent that include granite-greenstone belts older than 3.3 Ga. The age data from each craton are from the tonalite-trondjhemite-granodiorite complexes (e.g., Singhbhum craton [Misra et al. 1999] and Bastar craton [Ghosh 2004]) and from felsites of the metasedimentary successions (Dharwar craton; Naqvi 2005, p. 16). *B*, Generalized geological map of the Precambrian of the Singhbhum craton.

strain and weakly metamorphosed, similar to the Coonterunah Group (Buick et al. 1995; Green et al. 2000; Van Kranendonk et al. 2002) and parts of the Theespruit Formation (Viljoen and Viljoen 1969), and it provides a new insight into tectonics and surface processes on Earth at 3.5 Ga. The IOG succession also contains a thick (~120 m) oxide facies banded iron formation (BIF), which has additional implications for redox conditions on early Earth.

Geological Background

The early Archean Dharwar, Singhbhum, and Bastar cratonic nuclei in India (fig. 1*A*) include granite-greenstone terrains as old as ~3.34–3.56 Ga, as documented by 3.56-Ga Pb-Pb zircon ages for tonalite-trondjhemite-granodiorite gneisses of the Bastar craton (Ghosh 2004) and ~3.34-Ga felsites of the Dharwar craton (Naqvi 2005, p. 16). Evidence of earlier crust is recorded in ~3.58-Ga detrital zircons of supracrustal rocks of the Dharwar craton (Nutman et al. 1992; Peucat et al. 1995) and ~3.6-Ga detrital zircons in metasediments of the Older Metamorphic Group (OMG) of the Singhbhum craton (Goswami et al. 1995). Apart from the OMG, the Singhbhum craton (fig. 1*B*) includes extensive greenstone belt successions, collectively known as the IOG, and is composed of BIF up to 120 m thick, mafic-felsic volcanic rocks, chert, shale, and carbonate (Jones 1934; Acharyya 1993; Saha 1994; Mukhopadhyay 2001). These BIF-bearing volcano-sedimentary successions are exposed along the western, eastern, and southern perimeters of the Singhbhum granitoid and are informally known as the western, eastern, and southern IOG, respectively (fig. 1*B*). Thus far, no direct age has been determined for any of the three IOG successions. A minimum age of ~3.2 Ga is provided by granitoids intrusive into the three main greenstone belts (cf. Paul et al. 1991; Misra 2006). However, there are indications that some of the greenstone material may be older than 3.44 Ga. For example, the so-called older metamorphic tonalite gneiss, with an age of 3.44 Ga (Misra et al. 1999), intrudes small rafts of deformed and metamorphosed greenstone material, including BIF, in the central part of the Singhbhum granitoid batholith complex (fig. 1*B*). The dacitic volcanic rocks dated during this study come from the southern IOG (fig. 1*B*).

Southern IOG

The stratigraphic succession of the southern IOG is well exposed along the Tamka-Daitari Range (Chakraborty et al. 1980; Acharya 2002) and belongs to the southern limb of a large E-W trending, westerly plunging anticlinal structure. The succession, which consists from the base upward of massive and pillowed basalts with a few thin (2–5 m thick) gray to green chert interbeds, felsic to intermediate volcanic and volcaniclastic rocks (tuffs), bedded chert, and BIF (fig. 2), is weakly deformed and, for the most part, has undergone only greenschist-facies metamorphism. Localized zones of amphibolite-grade metamorphism appear to be related to the proximity of the intrusive Singhbhum granite (Saha 1994), and intense structural deformation is restricted to some shear zones. The result is that primary depositional/diagenetic features are

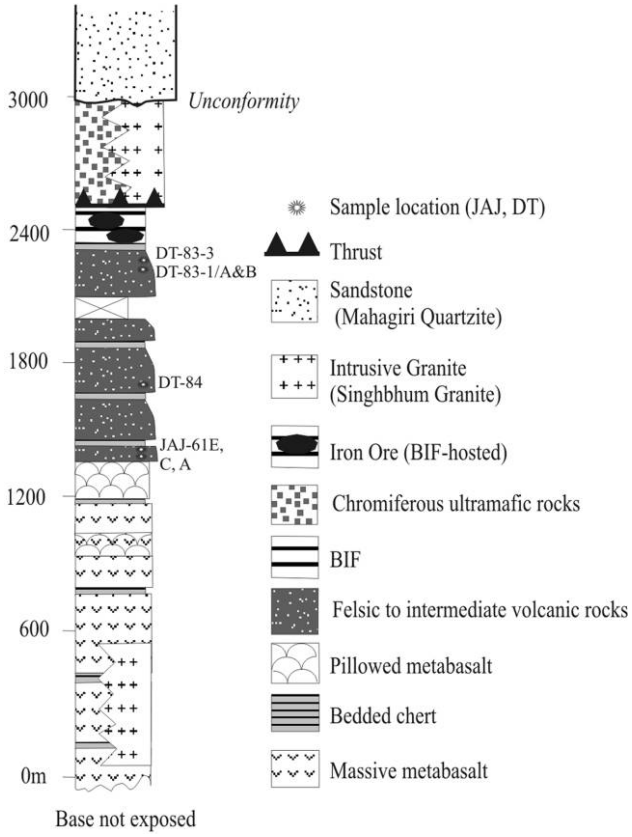

Figure 2. Composite lithologic log of the southern Iron Ore Group around Daitari Mining Township. Positions of samples are shown.

commonly well preserved in the BIF, bedded chert, and tuffs. Locally, a podiform chromiferous ultramafic body (Augé et al. 2003; Mondal et al. 2006, 2007) overlies the BIF with a thrust contact (cf. Banerjee 1997). Together, the ultramafic body and the granite-greenstone succession are unconformably overlain by a thick siliciclastic shelf succession, the Mahagiri Quartzite (fig. 2), that includes detrital chromite grains in its lower part and is considered to be of Paleoproterozoic age (Saha 1994).

The lower massive to pillowed (fig. 3*A*) basalt unit of the greenstone belt succession is overlain by a ~10-m-thick dacitic lava (fig. 3*B*), i.e., the unit that was sampled and dated in this study. The lava typically displays feldspar phenocrysts in a slightly recrystallized and weakly cleaved quartzose-sericitic groundmass. Feldspars are essentially orthoclase/microcline, with subordinate albite. The contact between the basalt and the dacitic lava is not well exposed in the sampled section. However, pillow basalt occurs a few meters below the dacitic lava. The dacitic lava is sharply overlain by ~3-m-thick gray and black bedded chert, which, in turn, is overlain by a thick pile of felsic to intermediate volcaniclastic rocks with interbeds of gray to black bedded chert. The volcaniclastic rocks, now in part metamorphosed to quartz-sericite schists, mainly represent massive sandy debris flows to plane, parallel-bedded, normally graded, fine-grained turbiditic subaqueous tuffs (fig. 3*C*). They are devoid of wave-generated primary sedimentary structures. Some beds are vesiculated. On the basis of consistent upward directions in pillow basalt below the dacitic lava and graded beds in volcaniclastic rocks above, we are confident that the succession is normal and conformable, without major stratigraphic or tectonic breaks.

The volcaniclastic rocks overlying the dacitic lava grade upward through gray bedded chert into a ~120-m-thick BIF. The transition is very well exposed in the Daitari Iron Ore Mine area, and it is possible to traverse continuously from the sample site into the BIF without break. The BIF displays well-preserved mesobanding defined by alternating iron- and chert-rich bands (fig. 3*D*). It includes both oxide and carbonate facies members. The iron carbonates are now largely oxidized to goethite and/or hematite, but locally remnant carbonate is preserved. The iron oxides are mostly hematite after magnetite, i.e., martite. However, cryptocrystalline and microcrystalline hematites are present in chert mesobands as inclusions in microcrystalline quartz (fig. 3*E*, 3*F*). These hematites appear to be the earliest-formed oxide phase and have been partly converted to magnetite during diagenesis or low-grade metamorphism. The magnetites, in turn, were transformed to martite during recent supergene alteration.

Geochemistry

For the compositional and tectonic characterization of the volcanosedimentary succession dated here, geochemical analyses were obtained from three samples of the dacitic flow (JAJ-61A, JAJ-61C, and JAJ-61E) that have been dated, one from another lava flow (DT-84) from the middle and three samples of volcaniclastic rocks (DT-83/1A, DT-83/1B, and DT-83-3 in table 1) from the upper parts of the succession (fig. 2). Details of analytical procedures are as follows.

X-ray fluorescence (XRF) analyses of all the samples were carried out on a Magix XRF spectrometer operated at 4 kV at the University of Johannesburg. Trace element compositions for three samples, DT-83/1A, DT-83/1B, and DT-84, were analyzed by instrumental neutron activation analysis (INAA)

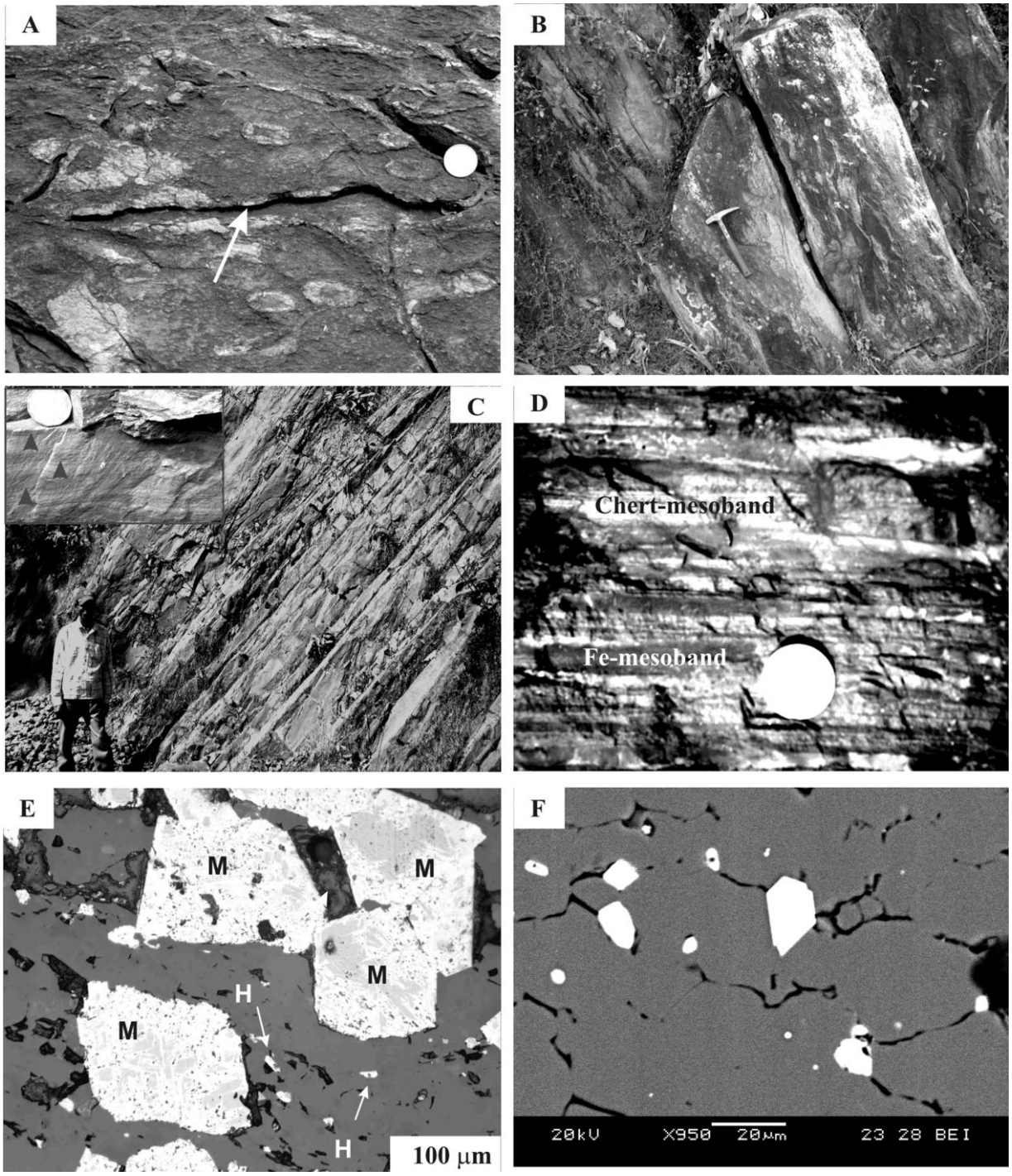

Figure 3. *A*, Pillowed metabasalt from the basic volcanic unit at the lower part of the greenstone succession. Note preserved chilled margin (*arrow*) of the pillow structure. *B*, Thickly bedded massive dacitic lava (sampled for geochronology) from the base of the felsic to intermediate volcanic interval. *C*, Medium- to thin-bedded fine-grained felsic tuffs. Note plane, parallel bedding characteristic of deep-water turbidite deposits. *Inset*, Normally graded turbidite beds (*arrowheads*) in a small handsample of felsic tuff. Coin diameter = 2.5 cm. *D*, Partially oxidized banded iron formation (BIF) from Tamka hill section. Note well-preserved Fe (*darker*) and chert/jasper (*lighter*) mesobands. Coin diameter = 2.5 cm. *E*, Reflected-light optical micrograph of oxide-facies BIF under plane-polarized light. Note presence of coarse euhedral martites (*M*) after magnetite and microcrystalline/cryptocrystalline hematites (*H*) in chert (*dark gray*) groundmass. *F*, SEM backscattered electron image of cherty mesobands in the BIF showing crypto- to microcrystalline hematite within microcrystalline quartz. The cryptocrystalline dusty hematite inclusions are likely to represent the earliest-formed hematite phase in the BIF.

at ACTLABS, Ontario, Canada. The procedure for analyses with INAA (described in detail at http://www.acmelab.com) was standardized at ACTLABS, where sample powders were dissolved in lithium metaborate flux and the resultant bead rapidly digested in dilute nitric acid. INAA precision and accuracy based on replicate analysis of international rock standards were 2%–5% (1 s) for most elements and ±10% for U, Sr, Nd, and Ni. Four samples, JAJ-61A, JAJ-61C, JAJ-61E, and DT-83-3, were analyzed for trace elements at the National Geophysical Research Institute (NGRI), Hyderabad, India, with a PerkinElmer SCIEX ELAN DRC-II inductively coupled plasma mass spectrometer (ICPMS; Concord, Ontario), following Balaram and Gnaneshwar Rao (2003). The precision and accuracy based on replicate analysis of international rock standards were 2%–5% (1 s) for most elements. The analyses were controlled by measurements of certified international standards (JR 1 and JR 2).

Glass beads were prepared for the XRF analyses by fusing sample powder into a borate glass. One gram of sample powder was mixed with 1 g flux (50% Li metaborate and 50% Li tetraborate). Samples were fused in an induction-heated Pt crucible. The measurements were monitored by several internal and international standards. Detection limits of major and trace elements for the XRF analyses were 250 ppm for SiO_2; 20 ppm for TiO_2 and P_2O_5; 150 ppm for Al_2O_3 and Fe_2O_{3t}; 15 ppm for Mn; 65 ppm for MgO and Na_2O; 40 ppm for CaO; 50 ppm for K_2O; 13 ppm for Ba; 1 ppm for Rb, Sr, Ni, Cu, Zr, Y, Pb, and Nb; and 3 ppm for V. Detection limits for the INAA analyses of trace elements were 1 ppm for Co, Mo, Cs, and Hf; 0.3 ppm for Ta; 0.1 ppm for Sc; 0.2 ppm for Th; and 0.5 ppm for U. The detection limits were found to be <0.005 ppb for almost all the elements determined by ICPMS at the NGRI laboratory. All values are based on the data obtained by the multielement peak hopping mode.

The analyses indicate that the volcanic rocks are felsic in composition, with SiO_2 concentrations between 66% and 80% (table 1). The relatively high alumina content, variable soda/potash ratio, and sericitic groundmass suggest that the rocks have undergone metasomatic and sericitic alteration similar to what has been reported from some of the oldest greenstone successions, e.g., the Barberton Greenstone Belt (Lowe and Byerly 1999). Samples of dacitic lava (JAJ-61A, JAJ-61C, and JAJ-61E in table 1) are generally richer in Na_2O and have lower concentrations of K_2O, which correlates with enrichment in Al_2O_3, relative to the volcaniclastic rock samples (table 1). Using quantitative estimates of the intensity of alteration with the alteration box plot for magmatic and especially volcanic rocks (Large et al. 2001), we find that the samples plot outside of the unaltered fields for rhyolites (fig. 4*A*). The volcaniclastic samples underwent stronger sericitization and K-feldspar alteration than did the lava samples dated here, probably because of hydrothermal processes (fig. 4*A*). The dacitic lava samples used for dating are less affected by alteration and point to a different trend with alteration products such as K-feldspar and albite (fig. 4*A*), likely formed during low-grade metamorphism and not by hydrothermal processes (cf. Gifkins et al. 2005). The significant alteration requires an igneous rock classification scheme for altered and older rocks, with the ratio of immobile trace elements such as Nb/Y versus Zr/Ti (e.g., Winchester and Floyd 1977), in which most samples fall within the dacite-rhyodacite field (but two samples straddle the line to trachyandesites; fig. 4*B*). Using immobile trace elements such as Ta, Nb, Yb, Zr, and Y, we may obtain data on the tectonic setting for these volcanic rocks. In the Ta-Yb discrimination diagram, the dacitic lava and tuff samples fall in the volcanic arc granite field (fig. 4*C*; fields are after Pearce et al. 1984). The samples in the Nb/Y versus Zr/Y diagram (fig. 4D; fields after Condie 2005) also suggest affinity to a volcanic arc setting and a nonplume source (cf. Kerrich et al. 2008).

Geochronology

Two fresh samples, JAJ-61A and JAJ-61E, were collected from the base and the top of the ~10-m-thick dacitic lava unit (21°06′27.3"N, 85°49′37"E) in a roadcut along the main mine road in the township of Daitari (figs. 2, 3*B*). Zircon grains were separated at the Research School of Earth Sciences (RSES) at the Australian National University by using standard magnetic and heavy-liquid techniques. The zircons, together with the reference zircons FC1 (Paces and Miller 1993) and SL13, were mounted in epoxy. All zircons were photographed in transmitted and reflected light, and these, together with SEM cathodoluminescence images, were used to decipher the internal structures of the sectioned grains and to target specific areas within the zircons for spot analysis. U-Pb analyses were done using the SHRIMP II instrument at the RSES. Six scans of data through the masses $^{196}Zr_2O$, ^{204}Pb, background (at mass 204.1), ^{206}Pb, ^{207}Pb, ^{208}Pb, ^{238}U, ^{248}ThO, and ^{254}UO were collected for each analysis. Common Pb was insignificant in all analyses but was corrected for using the measured ^{204}Pb and assuming the relevant com-

Table 1. Major and Trace Element Composition of Selected Dacitic Lava and Volcaniclastic Rock Samples

Major elements (wt%)	SiO_2	Al_2O_3	Fe_2O_{3t}	MgO	CaO	Na_2O	K_2O	TiO_2	P_2O_5	MnO	LOI	Sum	CCPI	AI
DT-83/1A	79.9	11.2	1.44	.54	.01	.02	3.92	.37	.02	bdl	2.3	99.7	32	99
DT-83/1B	66.5	21.8	1.25	.93	.00	.61	6.17	.57	.02	bdl	3.2	101.0	23	92
DT-83-3	71.1	18.7	1.10	.71	.02	.03	6.41	.68	.02	bdl	3.0	101.8	21	99
DT-84	67.2	22.0	.49	.47	.18	.43	4.89	.68	.12	.01	1.9	98.3	15	90
JAJ-61A	78.4	13.3	.73	.39	.43	4.37	1.14	.31	.07	.02	1.5	100.7	16	24
JAJ-61C	71.6	16.4	.76	.68	.77	4.59	2.08	.39	.1	.02	.6	98.0	17	34
JAJ-61E	76.0	14.3	.89	.47	.72	4.56	1.33	.34	.09	.02	.8	99.5	18	25

Trace elements (ppm)	Ba	Rb	Sr	Cs	Cr	V	Ni	Co	Cu	Nb	Ta	Y	Zr	Hf	Sc	Th	U	Pb	Ga	Zn
DT-83/1A	86	86	19	2.0		37.7	34.5	4.3	6	8.8	.7	13.2	122	3.0	7.6	4.7	.90	9.9	14	22
DT-83/1B	163	125	16	3.0		57.2	34.6	2.3	3	12.8	.9	20.2	176	5.0	12	6.9	1.00	2.1	21	25
DT-83-3	111	104	7	1.6	9	1.0	1.3	1.0	2	4.6	.4	12.4	157	3.7	7.8	6.5	.02	22	19	42
DT-84	1865	103	65	2.5	17	1.1	1.5	2.3	4	3.1	.3	8.8	125	2.7	8.1	4.3	.02	269	20	45
JAJ-61A	595	29	113	1.0	9	.7	1.0	65.3	2	4.3	.5	10.8	111	2.7	5.4	4.8	.12	18	13	32
JAJ-61C	1152	62	170	2.0	9	1.0	1.5	24.6	2	4.4	.9	14.8	170	4.2	7.6	8.3	.05	241	25	31
JAJ-61E	823	33	113	1.0	8	.7	1.4	50.7	3	3.7	.8	17.9	144	3.2	4.9	5.5	.07	254	16	34

Note. bdl = below detection limit; CCPI = chlorite-carbonate-pyrite index; AI = Ishikawa alteration index.

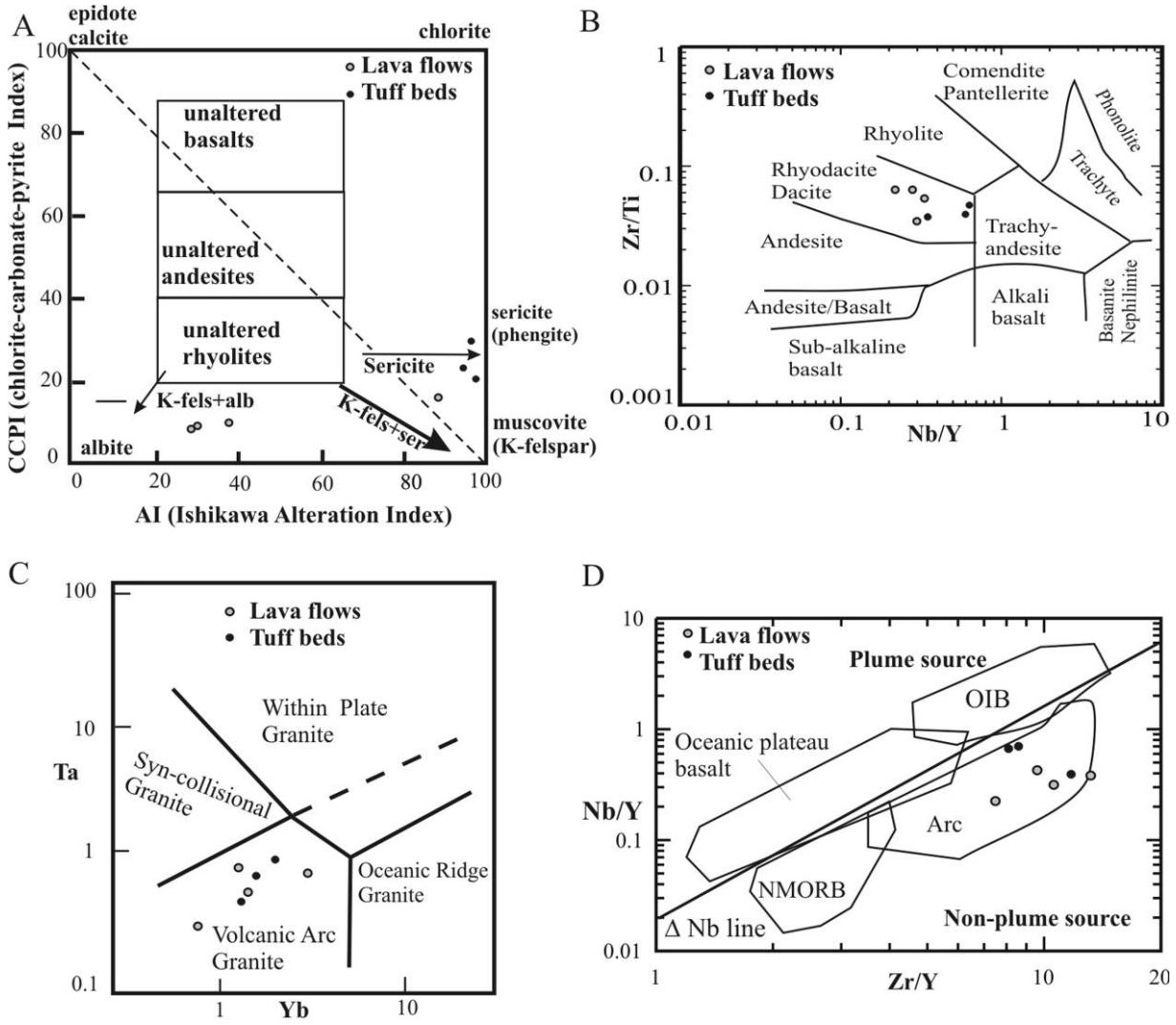

Figure 4. Characterization of the dacitic lava and volcaniclastics rocks (tuffs) based on major and trace element composition of selected samples. *A*, Alteration boxplot (after Large et al. 2001) of selected dacitic lava samples (JAJ; *gray circles*) and tuffs (DT; *black circles*). Note that the lava samples (with "JAJ-" prefix in table 1) dated here show a relatively lesser degree of alteration (K-feldspar and albitization) under diagenetic and low-grade metamorphic conditions; tuff samples and one lava sample show a higher degree of alteration (K-feldspar + sercitization) under hydrothermal conditions (alteration fields and trends are after Large et al. 2001). *B*, Classification of the lava and tuffs based on Zr/Ti and Nb/Y ratio plots (after Winchester and Floyd 1977). Note that both lava and tuff samples plot in the dacite-rhyodacite field. *C*, Ta/Yb discrimination diagram for the dacitic lava and tuff samples. Note that all samples plot in the tectonic field of volcanic arc granite (fields are after Pearce et al. 1984). *D*, Nb/Y versus Zr/Y discrimination diagram for the dacitic lava and tuff samples. Note that samples of both lavas and tuffs display arc affinity and nonplume sources. *NMORB* = normal mid-ocean ridge basalts; *OIB* = ocean island basalts; *Arc* = arc-related basalts. The ΔNb line separates plume from nonplume basaltic sources. Fields are after Condie (2005) and Kerrich et al. (2008).

position of the Stacey and Kramers (1975) model. The data have been reduced in a manner similar to that described by Williams (1998 and references therein), using the SQUID Excel macro of Ludwig (2001). Uncertainties given for individual U-Pb analyses (ratios and ages) are at the 1σ level; however, the uncertainty in the calculated concordia age (calculated using SQUID) is reported at the 95% confidence level and includes the uncertainties in the standard calibration. The data are plotted using Isoplot/Ex 3 software (Ludwig 2003).

The zircon crystals extracted from the dacitic lava are dark pink and anhedral to subhedral. Most grains display strong oscillatory-zoned growth, and a few show small, unzoned centers. Apart from two analyses (4.1 and 10.1), all data (fig. 5; table 2) plot

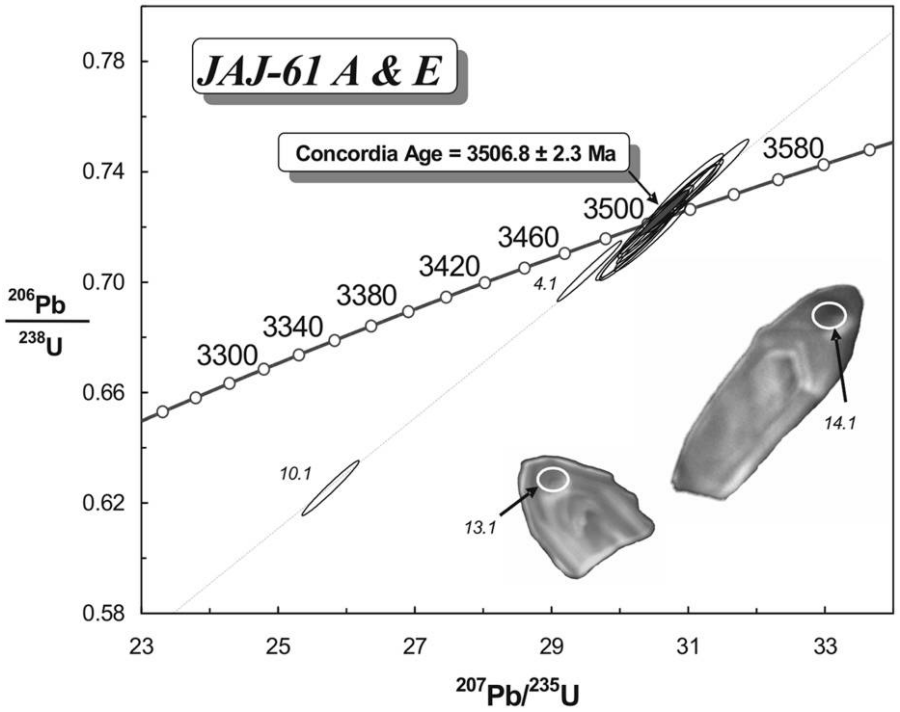

Figure 5. Concordia plot of SHRIMP U-Pb zircon data for the southern Iron Ore Group dacitic lava. Individual error ellipses are 1σ. Note cathodoluminescence-SEM images of some euhedral zircons with ~20-µm-diameter analytical spots marked.

within error of concordia and combine to give a concordia age of 3506.8 ± 2.3 Ma (fig. 5). Analyses were mainly sited in the oscillatory-zoned (magmatic) tips of the zircon grains, with a few sited in the more central parts of the grains. The results show that the zircons are all part of a uniform coeval population and that no inherited cores were detected. The date of 3506.8 ± 2.3 Ma is therefore considered to be the best estimate of the age of emplacement of this lava.

Geological Significance

The 3506.8 ± 2.3-Ma dacitic lava represents the oldest-dated rock unit of the Singhbhum craton and of any greenstone belt in India. The age of the lava also indicates that the southern IOG is one of the oldest greenstone successions in the world that is not highly strained and metamorphosed. Other greenstone belt successions with preservation similar to that of the southern IOG are all younger, with the exception of the slightly older Coonterunah Group (~3.515 Ga; Buick et al. 1995) in the Pilbara craton, Western Australia. The Theespruit Formation and related units in the Barberton area, South Africa, are comparable to or are slightly older in age than the southern IOG but are mostly amphibolite grade, commonly sheared, and cut by numerous unresolved faults and only rarely contain well-preserved low-strain enclaves (Viljoen and Viljoen 1969; Lowe 1999). The other well-preserved successions from the Warrawoona Group of the Pilbara craton in Western Australia (Buick and Dunlop 1990; Thorpe et al. 1992; Barley 1993; Krapez 1993) are in the order of 3.4–3.48 Ga. Recently, Furnes et al. (2007) described a vestige of the oldest ophiolitic crust from the sheeted dike complex of the ~3.8-Ga Isua Greenstone Belt. However, these older ~3.7–3.8-Ga successions in West Greenland, northern Labrador, and northern Quebec are so strained and metamorphosed to amphibolite and higher grade (Nutman et al. 1989, 1997, 2004; Dauphas et al. 2007) that inferences drawn from them about stratigraphic relationships and early Earth systems are often controversial (see review in Myers and Crowley 2000; Hamilton 2007).

The oldest well-preserved greenstone succession in the Coonterunah Group is dominantly composed of basalt, gabbro, rhyolitic to andesitic volcanics, and minor sedimentary units such as carbonates and ferruginous chert (Green et al. 2000; Van Kranendonk et al. 2002, 2007; Smithies et al.

Table 2. Summary of SHRIMP U-Pb Zircon Data for Samples of Dacitic Lava (JAJ-61A and JAJ-61E) of the Southern Iron Ore Group, Singhbhum Craton, India

Grain spot	Percent $^{206}Pb_c$	U (ppm)	Th (ppm)	$^{232}Th/^{238}U$	$^{206}Pb^*$ (ppm)	$^{206}Pb/^{238}U$ age[a]		$^{207}Pb/^{206}Pb$ age[a]		Percent discordant	$^{207}Pb^*/^{206}Pb^*$ (±%)[a]	$^{207}Pb^*/^{235}U$ (±%)[a]	$^{206}Pb^*/^{238}U$ (±%)[a]	Err corr[b]
1.1	.00	119	102	.89	75.0	3546.6	31.4	3500	5	−1	.3057 (.3)	30.92 (1.2)	.7335 (1.2)	.966
2.1	.00	177	83	.49	108.5	3470.7	29.8	3510	4	1	.3078 (.3)	30.27 (1.1)	.7133 (1.1)	.975
3.1	−.01	165	79	.49	101.5	3483.1	30.0	3513	4	1	.3084 (.3)	30.47 (1.1)	.7166 (1.1)	.973
4.1	.01	392	137	.36	237.3	3437.6	28.0	3493	3	2	.3044 (.2)	29.57 (1.1)	.7045 (1.1)	.987
5.1	.02	180	97	.56	112.9	3539.0	30.2	3505	4	−1	.3068 (.3)	30.95 (1.1)	.7315 (1.1)	.975
6.1	.00	178	93	.54	112.9	3567.4	30.4	3507	4	−2	.3072 (.2)	31.31 (1.1)	.7391 (1.1)	.976
7.1	.00	330	203	.64	203.7	3491.3	28.6	3507	3	0	.3073 (.2)	30.45 (1.1)	.7187 (1.1)	.985
8.1	.01	150	71	.49	92.2	3469.7	30.1	3507	4	1	.3071 (.3)	30.19 (1.2)	.7130 (1.1)	.971
9.1	.00	153	163	1.10	96.2	3537.2	30.6	3504	4	−1	.3067 (.3)	30.91 (1.2)	.7310 (1.1)	.973
10.1	.08	298	164	.57	160.2	3130.6	26.5	3463	3	10	.2985 (.2)	25.73 (1.1)	.6252 (1.1)	.981
11.1	.00	145	65	.46	90.8	3531.4	30.8	3509	4	−1	.3076 (.3)	30.94 (1.2)	.7295 (1.1)	.971
12.1	.01	121	46	.39	74.3	3473.0	31.9	3509	5	1	.3076 (.3)	30.27 (1.2)	.7139 (1.2)	.966
13.1	.03	136	62	.47	84.5	3508.7	30.9	3503	5	0	.3065 (.3)	30.57 (1.2)	.7234 (1.1)	.969
14.1	.02	156	63	.42	96.5	3502.1	30.4	3505	4	0	.3067 (.3)	30.52 (1.2)	.7216 (1.1)	.971

Note. Errors are 1σ; Pb_c and Pb^* indicate the common and radiogenic portions, respectively. Error in standard calibration was 0.21% (not included in above errors but required when comparing data from different mounts). SHRIMP analyses were performed at the Research School of Earth Sciences, Australian National University.

[a] Common Pb corrected using measured ^{204}Pb.

[b] Error correlation.

2007). On the basis of geochemical evidence from the basalts of the Coonterunah Group, Green et al. (2000) suggested that the greenstones were erupted on a continental basement. In contrast, the 3.51-Ga southern IOG greenstone belt succession consists of mafic to intermediate and felsic volcanic rocks with thick BIF. Our initial investigations suggest that the volcanic rocks of the southern IOG succession may well have formed in a volcanic arc environment similar to what is reported from some other Archean greenstone belt successions (Komiya et al. 1999; Polat and Frei 2005; Kerrich et al. 2008).

The other important aspect of the southern IOG succession is the presence of a very prominent BIF unit. This thick iron formation may well represent the oldest-known low-grade metamorphic iron formation. Although it has not been directly dated, the iron formation conformably overlies the felsic to intermediate volcanic pile in the southern IOG, which could place it at ~3.5 Ga. The oldest prominent iron formations in the low-grade metamorphic Barberton and Pilbara greenstone belts are ~3.44 Ga (Trendall 2000; Tice and Lowe 2004; Bolhar et al. 2005). Earlier ones in the 3.7–3.8-Ga greenstone belts of West Greenland, Labrador, and Quebec have all experienced at least amphibolite-grade metamorphism and commonly display disrupted tectonic contacts with adjacent lithologies (Nutman et al. 1989; Polat and Frei 2005; Dauphas et al. 2007). Most interestingly, the iron formation in the southern IOG preserved crypto- to microcrystalline hematite together with magnetite. All older iron formations contain only magnetite as an iron oxide phase (Dymek and Klein 1988; Nutman et al. 1989; Dauphas et al. 2007; Frei and Polat 2007), but this may be a function of their high metamorphic grade. In contrast, the oldest iron formation in the Barberton Greenstone Belt, the Buck Reef Chert, is composed of siderite (Tice and Lowe 2004). This led Tice and Lowe (2004) to propose that the siderite precipitated directly from carbonate-oversaturated ocean water under anaerobic atmospheric conditions with high CO_2 contents and no influence of microbial activity in the precipitation of the BIF. Obviously, this model cannot apply to the magnetite-hematite facies BIF that is dominant in the southern IOG. Here, either free oxygen must have been available in the water column to precipitate hematite or it was precipitated by anaerobic iron-oxidizing photosynthetic bacteria (Beukes 2004; Kappler and Newman 2004; Kappler et al. 2005). Up to now, it has not been possible to unequivocally differentiate between the latter two possibilities of hematite precipitation. However, the general lack of organic matter in iron formations, including those of the southern IOG, may favor the notion that anaerobic photosynthetic iron-oxidizing bacteria were not involved in precipitation of hematite-rich BIF and hence imply great antiquity of oxygenic photosynthesis (Beukes 2004; Rosing and Frei 2004).

ACKNOWLEDGMENTS

This work is a part of the Council of Scientific and Industrial Research, India, Major Research Project (extramural; no. 24[0280]/05/EMR-II to J. Mukhopadhyay and G. Ghosh). The analytical cost for the geochronology was funded by N. J. Beukes from a research grant of the National Research Foundation (Pretoria) under the Indo-South African Collaborative Program with the Department of Science and Technology (India). J. Mukhopadhyay, G. Ghosh, and R. A. Medda acknowledge hospitality extended by the Tata Steel, Sukinda, and Orissa Mining Corporation (India), Daitari. B. Armstrong, C. Magee, and S. Paxton of the Research School of Earth Sciences at Australian National University are thanked for their assistance in the sample preparation for the SHRIMP analyses. We also acknowledge the Geochemistry Division, National Geophysical Research Institute, Hyderabad, India, for the chemical analyses of the rock samples. The comments from A. Kröner and an anonymous reviewer greatly improved the manuscript.

REFERENCES CITED

Acharya, S. 2002. The Daitari-Tomka Basin: its structural and stratigraphic evolution and genesis of associated iron ores. Indian J. Geol. 74:49–81.

Acharyya, S. K. 1993. Greenstones from Singhbhum craton, their Archaean character, oceanic crustal affinity and tectonics. Proc. Natl. Acad. Sci. India A 63:211–222.

Armstrong, R. A.; Compston, W.; de Wit, M. J.; and Williams, I. J. 1990. The stratigraphy of the 3.5–3.2 Ga Barberton Greenstone Belt revisited: a single zircon ion microprobe study. Earth Planet. Sci. Lett. 101: 90–106.

Augé, T.; Cocherie, A.; Genna, A.; Armstrong, R.; Guerrot, C.; Mukherjee, M. M.; and Patra, R. N. 2003. Age of the Baula PGE mineralization (Orissa, India) and its implications concerning the Singhbhum Archaean nucleus. Precambrian Res. 121:85–101.

Balaram, V., and Gnaneshwar Rao, T. 2003. Rapid determination of REEs and other trace elements in geological samples by microwave acid digestion and ICP-MS. At. Spectrosc. 24:206–212.

Banerjee, P. K. 1997. Geodynamic implications of chrome-poor enstatite bodies in the Sukinda-Baula-Nausahi ultramafic suites of Orissa. Proc. Indian Acad. Sci. (Earth Planet. Sci.) 106:357–360.

Barley, M. E. 1993. Volcanic, sedimentary and tectonostratigraphic environments of the ~3.46 Ga Warrawoona Megasequence: a review. *In* Blake, T. S., and Meakins, A. L., eds. Archean and early Proterozoic geology of the Pilbara region, Western Australia. Precambrian Res. 60:47–67.

Beukes, N. J. 2004. Biogeochemistry: early options in photosynthesis. Nature 31:522–523.

Bolhar, R.; Van Kranendonk, M. J.; and Kamber, B. S. 2005. A trace element study of siderite-jasper banded iron formation in the 3.45 Ga Warrawoona Group, Pilbara craton: formation from hydrothermal fluids and shallow water. Precambrian Res. 137:93–114.

Buick, R., and Dunlop, J. S. R. 1990. Evaporitic sediments of Early Archean age from the Warrawoona Group, North Pole, Western Australia. Sedimentology 37: 247–277.

Buick, R.; Thornett, J. R.; McNaughton, N. J.; Smith, J. B.; Barley, M. E.; and Savage, M. 1995. Record of emergent continental crust ~3.5 billion years ago in the Pilbara craton of Australia. Nature 375:574–577.

Chakraborty, K. L.; Chakraborty, T. L.; and Majumder, T. 1980. Stratigraphy and structure of the Precambrian banded iron formations and chromite-bearing ultramafic rocks of the Sukinda Valley, Orissa. J. Geol. Soc. India 21:398–404.

Compston, W.; Kinny, P. D.; Williams, I. S.; and Foster, J. J. 1986. The age and Pb loss behaviour of zircons from the Isua supracrustal belt as determined by ion microprobe. Earth Planet. Sci. Lett. 80:71–81.

Condie, K. C. 2005. High field strength element ratios in Archean basalts: a window to evolving sources of mantle plumes? Lithos 79:491–504.

———. 2007. The distribution of Paleoarchean crust. *In* Van Kranendonk, M. J.; Smithies, H.; and Bennet, C. V., eds. Earth's oldest rocks. Developments in Precambrian geology 15. Amsterdam, Elsevier, p. 9–18.

Dauphas, N.; Cates, N. L.; Mojzsis, S. J.; and Busigny, V. 2007. Identification of chemical sedimentary protoliths using iron isotopes in the >3750 Ma Nuvvuagittug supracrustal belt, Canada. Earth Planet. Sci. Lett. 254:358–376.

Dymek, R. F., and Klein, C. 1988. Chemistry, petrology, and origin of banded iron formation lithologies from the 3800 Ma Isua supracrustal belt, West Greenland. Precambrian Res. 39:247–302.

Frei, R., and Polat, A. 2007. Source heterogeneity for the major components of ~3.7 Ga banded iron formations (Isua Greenstone Belt, Western Greenland): tracing the nature of interacting water masses in BIF formation. Earth Planet. Sci. Lett. 253:266–281.

Furnes, H.; de Wit, M.; Staudigel, H.; Rosing, M.; and Muehlenbachs, K. 2007. A vestige of Earth's oldest ophiolite. Science 315:1704–1707.

Ghosh, J. G. 2004. 3.56 Ga tonalite in the central part of the Bastar craton, India: oldest Indian date. J. Asian Earth Sci. 23:359–364.

Gifkins, C.; Herrmann, W.; and Large, R. 2005. Altered volcanic rocks. Tasmania, Centre for Ore Deposit Research, University of Tasmania, 275 p.

Goswami, J. N.; Misra, S.; Wiedenback, M.; Ray, S. L.; and Saha, A. K. 1995. 3.55-Ga-old zircon from Singhbhum-Orissa Iron Ore craton, eastern India. Curr. Sci. 69: 1008–1011.

Green, M. G.; Sylvester, P. J.; and Buick, R. 2000. Growth and recycling of early Archaean continental crust: geochemical evidence from the Coonterunah and Warrawoona groups, Pilbara craton, Australia. Tectonophysics 322:69–88.

Hamilton, W. B. 2007. Comment on "Vestige of Earth's oldest ophiolite." Science 318:746.

Jones, H. C. 1934. The iron ore deposits of Bihar and Orissa. Geol. Surv. India Mem. 63:167–302.

Kappler, A., and Newman, D. K. 2004. Formation of Fe(III) minerals by Fe(II)-oxidizing photoautotrophic bacteria. Geochim. Cosmochim. Acta 68:1217–1226.

Kappler, A.; Pasquero, C.; Konhauser, K.; and Newman, D. K. 2005. Deposition of banded iron formations by anoxygenic phototrophic Fe(II)-oxidizing bacteria. Geology 33:265–268.

Kerrich, R.; Polat, A.; and Xie, Q. 2008. Geochemical systematics of 2.7 Ga Kinojevis Group (Abitibi), and Manitouwadge and Winston Lake (Wawa) Fe-rich basalt-rhyolite associations: backarc rift oceanic crust? Lithos 101:1–23.

Komiya, T.; Maruyama, S.; Masuda, T.; Nohda, S.; Hayashi, M.; and Okamoto, K. 1999. Plate tectonics at 3.8–3.7 Ga: field evidence from the Isua accretionary complex, southern West Greenland. J. Geol. 107: 515–554.

Krapez, B. 1993. Sequence stratigraphy of the Archean supracrustal-belts of the Pilbara Block, Western Australia. Precambrian Res. 60:1–45.

Kröner, A.; Hegner, E.; Byerly, G. R.; and Lowe, D. R. 1992. Possible terrane identification in the early Archean Barberton Greenstone Belt, South Africa, using single zircon geochronology. EOS: Trans. Am. Geophys. Union 73:616.

Kröner, A.; Hegner, E.; Wendt, J. I.; and Byerly, G. R. 1996. The oldest part of the Barberton granitoid-greenstone terrain, South Africa: evidence for crust formation between 3.5 and 3.7 Ga. Precambrian Res. 78:105–124.

Large, R.; Gemmell, J. B.; and Paulick, H. 2001. The alteration box plot: a simple approach to understanding the relationship between alteration mineralogy and lithogeochemistry associated with volcanic-hosted massive sulfide deposits. Econ. Geol. 96: 957–971.

Lowe, D. R. 1999. Geologic evolution of the Barberton Greenstone Belt and vicinity. *In* Lowe, D. R., and

Byerly, G. R., eds. Geologic evolution of the Barberton Greenstone Belt, South Africa. Geol. Soc. Am. Spec. Pap. 329:287–312.

Lowe, D. R., and Byerly, G. R. 1999. Stratigraphy of the west-central part of the Barberton Greenstone Belt, South Africa. *In* Lowe, D. R., and Byerly, G. R., eds. Geologic evolution of the Barberton Greenstone Belt, South Africa. Geol. Soc. Am. Spec. Pap. 329:1–36.

Ludwig, K. R. 2001. SQUID 1.03: a user's manual. Berkeley Geochronology Center Special Publication 2. Berkeley, Berkeley Geochronology Center, 19 p.

———. 2003. Isoplot 3.00: a geochronological toolkit for Microsoft Excel. Berkeley Geochronology Center Special Publication 4. Berkeley, Berkeley Geochronology Center, 70 p.

Misra, S. 2006. Precambrian chronostratigraphic growth of Singhbhum-Orissa craton, eastern Indian shield: an alternative model. J. Geol. Soc. India 67:356–378.

Misra, S.; Deomurari, M. P.; Wiedenbeck, M.; Goswami, J. N.; Ray, S.; and Saha, A. K. 1999. $^{207}Pb/^{206}Pb$ zircon age ages and the evolution of the Singhbhum craton, eastern India: an ion microprobe study. Precambrian Res. 93:139–151.

Mondal, S. K.; Frei, R.; and Ripley, E. M. 2007. Os isotope systematics of Mesoarchean chromitite-PGE deposits in the Singhbhum craton (India): implications for the evolution of lithospheric mantle. Chem. Geol. 244: 391–408.

Mondal, S. K.; Ripley, E. M.; Li, C.; and Frei, R. 2006. The genesis of Archaean chromitites from the Nausahi and Sukinda massifs in the Singhbhum craton, India. Precambrian Res. 148:45–66.

Mukhopadhyay, D. 2001. The Archean nucleus of Singhbhum: the present state of knowledge. Gondwana Res. 4:307–318.

Myers, S., and Crowley, J. L. 2000. Vestiges of life in the oldest Greenland rocks? a review of early Archean geology in the Godthåbsfjord region, and reappraisal of field evidence for >3850 Ma life on Akilia. Precambrian Res. 103:101–124.

Naqvi, S. M. 2005. Geology and evolution of the Indian Plate (from Hadean to Holocene: 4 Ga to 4 Ka). New Delhi, Capital Publishing, 450 p.

Nutman, A. P.; Bennett, V. C.; Friend, C. R. L.; and Rosing, M. T. 1997. Approximately 3710 and ≥3790 Ma volcanic sequences in the Isua (Greenland) supracrustal belt: structural and Nd isotope implications. Chem. Geol. 141:271–287.

Nutman, A. P.; Chadwick, B.; Ramakrishnana, K.; and Viswanatha, M. N. 1992. SHRIMP U-Pb ages of detrital zircon in Sargur supracrustal rocks in western Karnataka, southern India. J. Geol. Soc. India 39:367–374.

Nutman, A. P.; Friend, C. R. L.; Barker, S. S.; and McGregor, V. R. 2004. Inventory and assessment of Palaeoarchaean gneiss terrains and detrital zircons in southern West Greenland. Precambrian Res. 135: 281–314.

Nutman, A. P.; Fryer, B. J.; and Bridgewater, D. 1989. The early Archaean Nulliak (supracrustal) assemblage, northern Labrador. Can. J. Earth Sci. 26:2159–2168.

Paces, J. B., and Miller, J. D. 1993. Precise U-Pb ages of Duluth Complex and related mafic intrusions, northeastern Minnesota: geochronological insights to physical, petrogenic, paleomagnetic and tectonomagmatic processes associated with the 1.1 Ga midcontinent rift system. J. Geophys. Res. 98B:13,997–14,013.

Paul, D. K.; Mukhopadhyay, D.; Pyne, T. K.; and Bishui, P. K. 1991. Rb-Sr age of granitoid in the Deo River section, Singhbhum, and its relevance to the age of iron formation. Indian Miner. 45:726–728.

Pearce, J. A.; Harris, N. B. W.; and Tindle, A. G. 1984. Trace element discrimination diagrams for the tectonic interpretation of granitic rocks. J. Petrol. 25:956–983.

Peucat, J. J.; Bouhaller, H.; Fanning, C. M.; and Jayananda, M. 1995. Age of the Holenarasipur Greenstone Belt, relationships with the surrounding gneiss, Karnataka, south India. J. Geol. 103:701–710.

Polat, A., and Frei, R. 2005. The origin of early Archean banded iron formations and of continental crust, southern West Greenland. Precambrian Res. 138: 151–175.

Rosing, M. T., and Frei, R. 2004. U-rich Archaean seafloor sediments from Greenland: indications of >3700 Ma oxygenic photosynthesis. Earth Planet. Sci. Lett. 217:237–244.

Saha, A. K. 1994. Crustal evolution of Singhbhum–North Orissa, eastern India. Geol. Soc. India Mem. 27, 341 p.

Smithies, R. H.; Champion, D. C.; and Van Kranendonk, M. J. 2007. The oldest well-preserved felsic volcanic rocks on Earth: geochemical clues to the early evolution of the Pilbara Supergroup and implications for the growth of a Paleoarchean protocontinent. *In* Van Kranendonk, M. J.; Smithies, H. R.; and Bennet, C. V., eds. Earth's oldest rocks. Developments in Precambrian geology 15. Amsterdam, Elsevier, p. 339–368.

Stacey, J. S., and Kramers, J. D. 1975. Approximation of terrestrial lead isotope evolution by a two-stage model. Earth Planet. Sci. Lett. 26:207–221.

Thorpe, R. I.; Hickman, A. H.; Davis, D. W.; Mortensen, J. K.; and Trendall, A. F. 1992. U-Pb zircon geochronology of Archean felsic units in the Marble Bar region, Pilbara craton. Precambrian Res. 56:169–189.

Tice, M. M., and Lowe, D. R. 2004. Photosynthetic microbial mats in 3,416-M-yr-old ocean. Nature 431: 549–552.

Trendall, A. F. 2000. Significance of banded iron formation (BIF) in the Precambrian stratigraphic record. Geoscientist 10:4–7.

Van Kranendonk, M. J.; Hickman, A. H.; Smithies, R. H.; and Nelson, D. R. 2002. Geology and tectonic evolution of the Archean North Pilbara Terrain, Pilbara craton, Western Australia. Econ. Geol. 97: 695–732.

Van Kranendonk, M. J.; Smithies, R. H.; Hickman, A. H.; and Champion, D. C. 2007. Paleoarchean development of a continental nucleus: East Pilbara Terrane of the Pilbara craton, Western Australia. *In* Van Kranendonk, M. J.; Smithies, H. R.; and Bennet, C. V., eds. Earth's oldest rocks. Developments in Precambrian geology 15. Amsterdam, Elsevier, p. 307–338.

Viljoen, M. J., and Viljoen, R. P. 1969. The geology and geochemistry of the Lower Ultramafic Unit of the Onverwacht Group and a new class of igneous rocks. Geol. Soc. S. Afr. Spec. Publ. 2:55–87.

Williams, I. S. 1998. U-Th-Pb geochronology by ion microprobe. *In* McKibben, M. A.; Shanks, W. C., III; and Ridley, W. I., eds. Applications of microanalytical techniques to understanding mineralizing processes. Rev. Econ. Geol. 7:1–35.

Winchester, A. F., and Floyd, P. A. 1977. Geochemical discrimination of different magma series and their differentiation products using immobile elements. Chem. Geol. 20:325–343.